J Mater Sci (2008) 43:384–389
DOI 10.1007/s10853-007-2182-9

Processing of nanocrystalline hydroxyapatite particles via reverse microemulsions

Hong Li · MinYing Zhu · LiHua Li · ChangRen Zhou

Received: 30 May 2006 / Accepted: 24 October 2006 / Published online: 6 October 2007

Abstract Nanocrystalline hydroxyapatite (HAP) particles were synthesized at room temperature using reverse microemulsions, in which cyclohexane was used as the organic phase, mixed surfactant with TX-100 and 1- pentanol, and $CaCl_2$ solution as aqueous phase. The reactor systems with aqueous/organic volumetric ratios 1:10, 1:5, 2:5, and 1:2 were carefully selected for the microemulsion processing by the pseudo-ternary phase diagram and the electric conductivity measurement of the emulsion. The as-obtained HAP nanoparticles with carbonate substitution and broadening X-ray diffraction (XRD) traces were similar to the fine powder of human bone, despite of the aqueous/organic volumetric ratio in the emulsion. No obvious other's phase occurred after as-obtained particles calcined under different temperature till 700 °C. In the emulsion-derived precursors, the HAP particles based on spherical morphology were prepared into the size between 15 ~ 30 nm as a low volumetric ratio of 1:10 or 1:5 was applied. As the volumetric ratio increased to 2:5, the HAP particles with rod-like shape of (140 ~ 280) × (10 ~ 80) nm were formed. Practical implication of the results is that the nanocrystalline bone-like hydroxyapatite can be obtained via the emulsion processing at room temperature without further calcinations.

Keywords Hydroxyapatite · Microelmusion · Nanocrystalline

H. Li (✉) · M. Zhu · L. Li · C. Zhou
Department of Materials Science and Engineering, Jinan University, Guangzhou 510632, China
e-mail: tlihong@jnu.edu.cn

Introduction

Synthetic hydroxyapatite (HAP) has excellent biocompatibility and bioactivity and has been widely used in many biomedical applications such as implants and coatings onto prostheses [1–3]. Besides its significant prospect in biology, it is also sought after in several multidisciplinary applications such as separating microseize filtering for heavy metals from aqueous solutions [4], proteins and nuclei acids in HPLC [5], and as immobilization of enzymes in biosystem engineering [6]. The function of HAP in all these applications is largely determined by its morphology, stoichiometry, crystallinity, and crystal size distribution. For example, nanosize HAP powders are sintering reactive, and the highly densified and refined microstructure derived from a nano-sized HAP powder can lead to a significant improvement in mechanical properties of sintered HAP, and therefore widens its applications as load-bearing implants [7, 8]. To coat HAP onto silicone substrate with covalent linkage, HAP particles with flat and wide plane are essentially necessary [9]. For HAP crystalline with partially substitution of CO_3^{2-} for OH^-, nanosized needle shape and 1.65 for the Ca/P atomic ratio, is the major mineral phase in bone [1], then HAP particles with chemically and structurally similar to the mineral portion of bone would be the most important step in obtaining a bone substitute. Especially for tissue engineering scaffold, HAP particles were processed into composites by blending with biopolymer, for to promote cell adhesion, migration, differentiation and proliferation [10–12], together with improving the mechanical strength.

A so-called bone-like apatite coating, which is carbonate-containing small crystallites and defective structure can produce by a biomimetic way [13]. HAP particles is chemically and structurally similar to the mineral portion

of bone are less formed, although various synthesis methods, including solid-state reaction [14], co-precipitation [15], and other processing [16–18], have been used for HAP particles. Most of these methods produce HAP particles with uncontrollable morphology, size and composition during drying or calcination at high temperature. Furthermore, HAP particles obtained by these processing usually cannot distribute uniformly when HAP particles blend into polymer, especially for oleophilic polymer.

Microemulsion has been shown to be one of the few methods being able to deliver a particle size and morphology in nanometer scale with minimum agglomeration. A emicroemulsion is a thermodynamically stable transparent solution of two immiscible liquids such as water (W) and organic (O) stabilized by an ampophilic surfactant. In case of a water-in-organic microemulsion, reverse micelles are formed when the aqueous phase is dispersed as microdroplets surrounded by a monolayer of surfactant in the continuous organic phase. These microdropltes of water act as nanoreactors in which reactions are conducted. It is noted that nano-sized HAP particles synthesized in water-in-organic microemulsions would be surrounded by a hydrophobic monolayer, and would be easy to distribute uniformly in polymer.

Microemulsion route had been successfully used in the development of fine HAP powders. Lim et al. reported submicrometer-sized HAP powder had been synthesized using cyclohexane as an organic phase, poly(oxyethylene)$_5$nonyl phenol ether(NP-5) and poly(oxyethylene)$_9$nonyl phenol ether (NP-9) as surfactant and the spherical HAP particles were obtained when the microemulsion-derived precursors were calcined at 650 °C [19]. Koumoulidis et al. used the microemulsion system of n-octane as continous hydrocarbon phase, cetyltrimethylammonium bromide (CTAB) as the surfactant, and 1-butanol as the cosurfactant to prepare the carbonated nano-size HAP with 40–120 nm after calcination at 635 °C, but the HAP particles were still aggregated particles [20]. In the mixing of NP-5 and NP-12 in cyclohexane, Susmita et al. reported that the particle morphology mainly depends on the shape of the micelle, and needle-like HAP particle would be obtained when a large aqueous/organic ratio was applied [21]. However, calcination was still applied in order to obtain crystalline HAP [19–23], while the size, composition, and morphology were altered. The processing also limited its application in preparing HAP/polymer composites for the hydrophobic monolayer surrounded by HAP particles had been burnt out during calcination.

In the present study, our effort is focused on the development of a synthetic route to produce nanocrystalline HAP with the similar structure and composition to HAP in bone at room temperature. A cyclohexane—mixed surfactant—aqueous solution system based on the previous report [24]. The HAP nanoparticles with chemically and structurally similar to the mineral portion of bone were synthesized at room temperature. The effect of aqueous/organic value on the structure of micelle was studied in detail. The emulsion-derived precursors containing HAP particles were observed by transmission electron microscopy (TEM). Particles obtained at different temperature were characterized using X-ray diffraction (XRD), Energy dispersive X-ray spectra (EDX) and Fourier-transform infrared attenuated total reflective spectroscopy (FT-IR). For EDX, the average Ca/P atomic ratio of each specimen was obtained in a number of three measurements.

Experimental

Materials

Analytical-grade chemicals $(NH_4)_2HPO_4$, $CaCl_2$, and ammonia solution were used as received. Polyethylene glycol octylphenyl ether (TX-100, $C_{34}H_{62}O_{11}$, chemical grade), and 1-pentanol (CH_3 $(CH_2)_4OH$, analytical grade) as supplied without further purification were the surfactant (S) and the assistant surfactant (A) respectively, together with cyclohexane (C_6H_{12}, analytical grade) as the continuous organic phase. Deionized water was used in each synthetic step. The human bone powders were donated by South China Medical University (Guangzhou, P.R. China).

Pseudo-ternary microemulsion system of cyclohexane—TX-100 and 1-pental—aqueous

For the microemulsion processing, the cyclohexane was used as the organic phase, and mixed (weight ratio 3:2) TX-100 (S) and 1-pentanol (A) as the surfactant phase. First, a cyclohexane—S+A—water phase diagram was established by a system titration based on the clear-turbid observation as described in reference [25–27]. Then, the electrical conductivity of the emulsion of cyclohexane—S+A—0.1 M $CaCl_2$ aqueous solution was measured according to reference [19, 28].

Synthesis of HAP particles

According to cyclohexane—S+A—water phase diagram, HAP particles were synthesized in the reaction system, which a volumetric ratio of 0.1 M $CaCl_2$ aqueous solution to organic phase is 1:10, 1:5, 2:5, and 2:1, respectively. Prepared stoichiometric 0.08 M NH_4OH and 0.06M$(NH_4)_2HPO_4$ aqueous water solution was added to

the emulsion stepwise with vigorous stirring for an hour at 30 °C. HAP formed as the following equation:

$$10CaCl_2 + 6(NH_4)_2HPO_4 + 8NH_4OH \rightarrow Ca_{10}(PO_4)_6(OH)_2 + 20\ NH_4Cl + 6H_2O$$

The emulsion-derived precursors were separated from the liquid phase by centrifugation, and washed three times with deionized water and pure ethanol. Finally, the precursors were dried at room temperature (30 °C) or 50 °C over night. Part of the samples calcined in an oven at 200, 650, and 700 °C, respectively under atmospheric pressure for 3 h.

Characterization

The electrical conductivity of emulsion was measured by DDS-11A (LEICI, Shanghai, P.R. China). The particles obtained at different temperature and the human bone powder were characterized by XRD (MASL, Beijing, P.R. China) and FTIR (EQUINOX 55, Bruker, Germany) respectively, while the KBr disk technique was employed for FTIR. A TEM (PHILIPS TECNAI-10, USA) was used to characterize the morphology of the emulsion-derived precursors without further treatment. EDX of the obtained particles were performed by IS/I-300, OXFORD, UK.

Results and discussion

Figure 1 shows the partial pseudo-ternary phase diagram for the system of cyclohexane—S+A—water at room temperature (30 °C). The microemulsion region is the shaded area, and any mixtures of cyclohexone, S+A, and water within this area are clear because of the small dispersion size of water droplets in the stable microemulsion. Out of this area, the mixtures are turbid. According to Fig. 1, composition point A consisting of 70 wt.% cyclohexane, 30 wt.% S+A would contain much more water in the system.

The clear-turbid observation could not differentiate a bicontinuous microemulsion from a reverse microemulsion. The compositions with a fixed S+A to cyclohexane weight ratio of 3:7 along the line across point A in Fig. 1 were characterized for electrical conductivity. At the same time, water phase was substituted by 0.1 M $CaCl_2$ aqueous solution. As the aqueous phase exhibits a much higher electrical conductivity than that of the organic phase of cyclohexane, a change in electrical conductivity will apparently indicate a change in the microstructure of the system [25, 28, 29]. For example, a water-in-organic

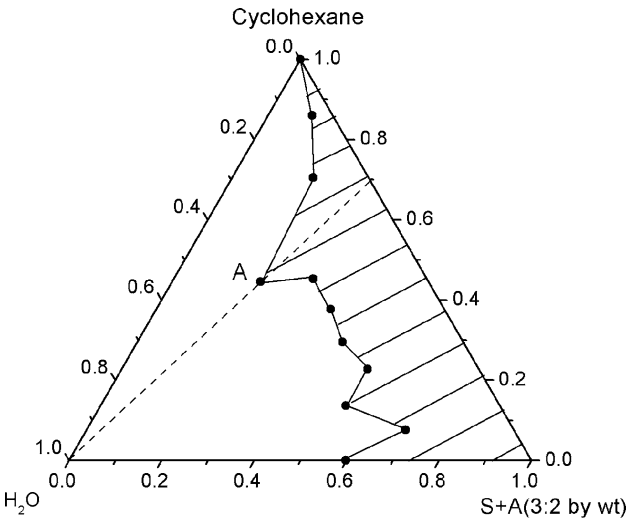

Fig. 1 The phase diagram established for cyclohexane / TX-100 + n-pentanol /water system (30 °C), the microemulsion region is marked as shaded area, here S+A denotes mixed surfactant and cosurfactant

microemulsion, in which the conducting aqueous phase is entrapped within the surfactant aggregates and occurs as isolated droplets in the organic matrix, will exhibit a low electrical conductivity. However, the aqueous phase dominates the electrical conductivity of the bicontinous emulsion or organic-in-water microemulsion, in which the conducting aqueous phase exists in the system, will sharply increase [25, 28, 29].

In our emulsion, the electrical conductivity appears to be low as shown in Fig. 2 when the aqueous solution/organic phase volumetric ratio drops below 1:5, then the water-in-organic micelle existed. As the ratio increases from 1:5 to

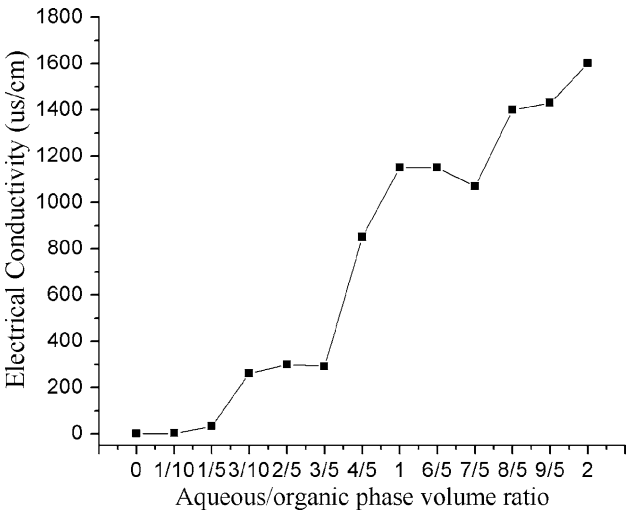

Fig. 2 The electrical conductivity as a function of 0.1 M $CaCl_2$ aqueous solution/organic in the composition of fixed (TX-100 + n-pentanol) to cyclehexone ratio of 3:7 (30 °C), as indicated by the dotted line in Fig. 1

3:5, the electrical conductivity shows little increment. It is implied that a transition of water-in-organic microemulsion to organic-in-water or bicontinuous emulsion was in process. When the volumetric aqueous/organic ratio reaches 1:2, the electrical conductivity increases dramatically, which indicates that the compositions are out of the microemulsion. Based on the investigation of Fig. 1 and Fig. 2, the volumetric ratios 1:10, 1:5, 2:5, and 1:2 of aqueous to organic were selected for the microemulsion processing in order to synthesize the nanocrystalline HAP particles in the water-in-organic micelles.

Figure 3 shows the TEM micrographs of nano-particles in different volumetric ratio of aqueous solution/organic after 0.08 M NH_4OH, and 0.06 M$(NH_4)_2HPO_4$ aqueous solution dissolving to the emulsion stepwise with stirring for an hour at 30 °C. The nano-size and agglomerate-free HAP particles with a narrow particle size distribution and different morphology were formed. Figure 3 (a) corresponds to the volumetric ratio 1:10 of aqueous/organic, and spherical nano-particles with about 15 nm disperse relatively equably. Figure 3(b) exhibits the nano-particles in the system of the volumetric ratio 1:5 of aqueous to organic, the size of nano-particles are about 25 ~ 35 nm and appear to be spherical. Rod-like particles were formed when aqueous/organic phase volumetric ratio was 2:5 in the emulsion, as shown in Fig. 3(c). The average size of the particles are within the range of 10 ~ 80 nm ×140 ~ 180 nm. The aspect ratio of the particles decreased as the aqueous/organic phase volume ratio reached 1:2, while the size of particles was larger than 90 nm. These phenomena are consistently in agreement with the results of Fig. 1 and Fig. 2. Surfactant, which dissolves in organic solvents form spherical aggregates, is called reverse micelle. The shape of the reverse micelle depends on the amount of water, organic phase, and surfactant and their ratio. According to the investigation of previous reports [26, 30], the micelle would rechange from spherical into rod-like particle as the aqueous/organic ratio increased. When the aqueous/organic ratio was as low as 1:10 and 1:5 in our experiment, the shapes of reverse micelles remain spherical in microemulsion. As a result, only spherical particles of HAP were obtained. As the aqueous/organic phase volumetric ratio increased further, the inside water pool was enlarged. The micelle size increased up to a dimension and even deformed their shapes to cylindrical micelle [30]. In this case, rod shape particles were produced. When micelle volume expanded further along with the increase of the aqueous/organic ratio, micelles broke up. The HAP nanoparticles formed in this system would aggregate, and then relatively larger particles were obtained as we studied. The results indicated that the size and morphology of HAP particles can be controlled to some extent, and rod-like HAP particles, whose morphology are similar to that of bone HAP, can be obtained when a relatively large aqueous/organic ratio is applied in a microemulsion.

Figure 4 shows the XRD patterns of the obtained samples via the microemulsion with different reaction system at room temperature. No obvious difference was observed, despite of the ratio of aqueous to organic phase. All peaks are attributed to HAP (File No.73–0293, International Centre for Diffraction Data, ICDD). The pH value of a reverse microemulsion was found to have a significant influence on the formation of HAP [1, 21, 26, 31, 32]. In our system, ammonium hydroxide solution was added before $(NH_4)_2HPO_4$ solution, so the emulsion maintains alkaline during the processing. Once the $(NH_4)_2HPO_4$ solution was added drop wise with continuous stirring, HAP was formed, which was consistent with the finding that HAP was formed in alkaline or neutral solution [1, 21].

Figure 5 shows the XRD patterns of the obtained samples heat-treated at 200, 650, 700 °C respectively and the human bone powder. As can be seen, the XRD patterns of

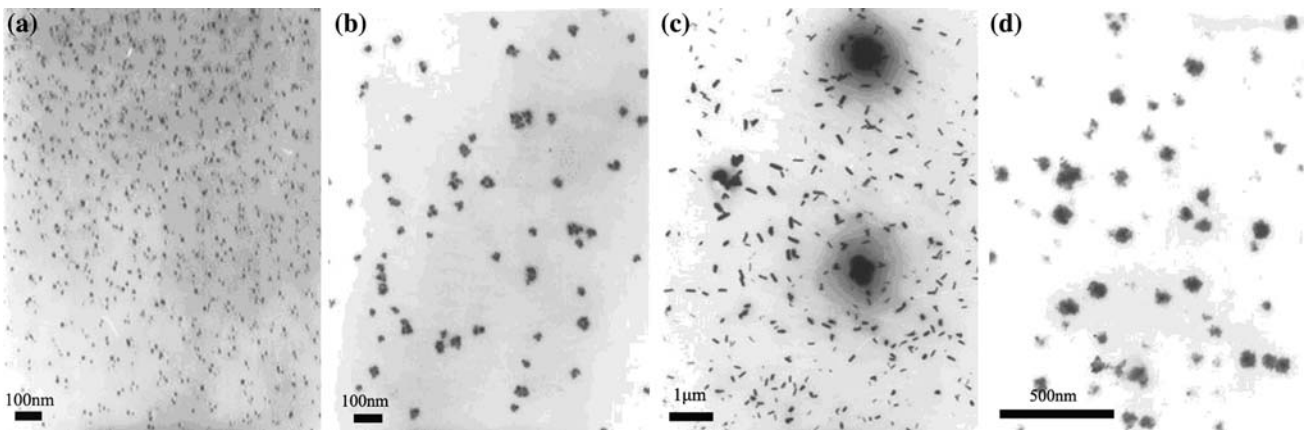

Fig. 3 TEM micrographs of the emulsion-derived precursors containing HAP nanoparticles in different volume ratios of aqueous/organic (**a**, 1:10; **b**, 1:5; **c**, 2:5; **d**, 1:2)

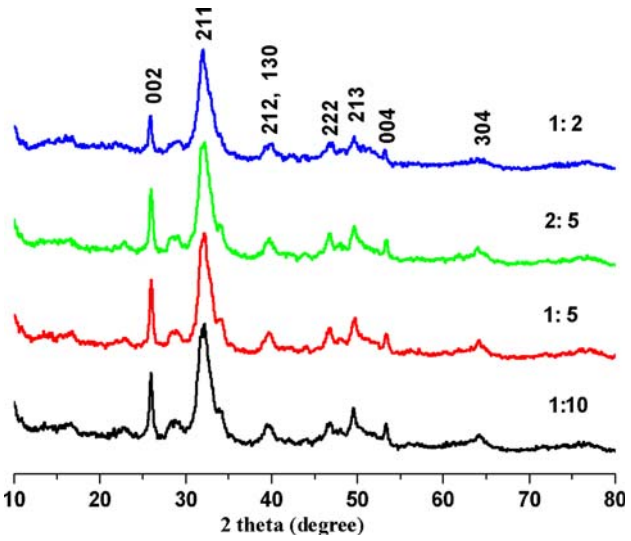

Fig. 4 XRD patterns of powders obtained from emulsion having 1:10, 1:5, 2:5, 1:2 aqueous/organic volume ratio

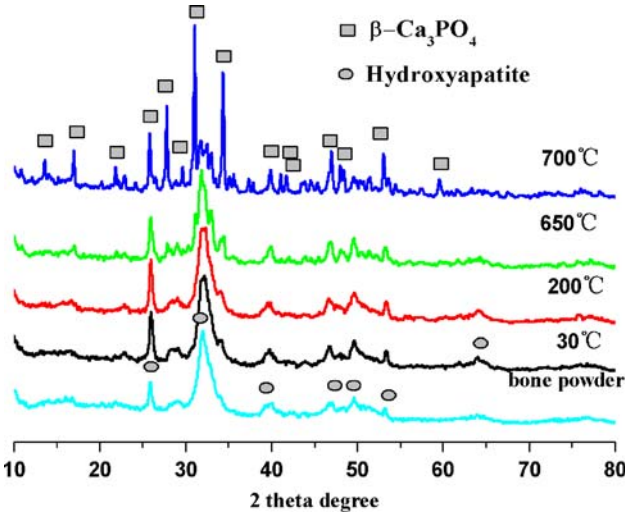

Fig. 5 XRD patterns of the human bone powder and the as-obtained powders treated at 30, 200, 600, and 700 °C

the samples as-received at 30 °C are similar to that of the human bone powder with relatively broad peaks and major peaks of crystalline HAP (File No.73-0293, ICDD). Due to peak-broadening of the XRD patterns, it is however difficult to estimate the presence of non-hydroxyapatite phases in the as-obtained samples. The EDX result (Fig. 6) of the as-prepared samples (1:5 for aqueous/organic, dried at 50 °C) shows the Ca/P atomic ratio is 1.658±0.002, slightly higher than that of human bone (1.65) [1]. The XRD pattern of the HAP powder calcined at 200 °C shows major peaks no obvious sharpen. After further calcination at 650 °C, the HAP powders exhibit more peaks attributed to HAP. No X-ray evidence was found for the existence of other calcium phosphate phases in the powder. Unlike

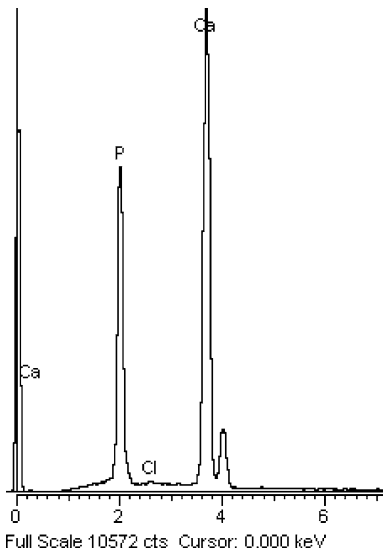

Fig. 6 EDX spectra of the obtained powder (1:5 for aqueous/organic, dried at 50 °C), the Ca/P atomic ratio is 1.658 according to the EDX spectra

others' study [19–22], further calcination processing achieved no dramatic improvement in crystallinity as can be seen from Fig. 5. These results imply that relatively high-purity crystalline HAP formed at room temperature (30 °C), and the relatively broadening peaks might attribute to the nano-size of HAP particles.

At approximately 700 °C, β-TCP (File No.70-2056, ICDD) is the main crystalline phase. The main reason for the transformation from HAP to β-TCP occurred at relatively low temperature maybe the nano-size of as-prepared HAP particles, for fine particle would be sensitive to heat treatment. Usually the Ca/P atomic ratio has a significant effect on the phase transformation from HAP to β-TCP [22]. However, HAP in bone with the atom ratio Ca/P of 1.65 was still HAP crystalline phase after calcined at 800 °C [1]. For the Ca/P of the samples is 1.658, it is hard to confirm whether the Ca/P had an effect on the transformation in the study. Therefore it is suspected that the transformation at relatively lower temperature resulted from the nano-size of the samples.

Figure 7 shows the infrared absorption spectra of the obtained samples phases and the human bone powders. The absorption bands at 3,570 and 633 cm^{-1}, respectively, correspond to the stretching vibration of the lattice OH^- ions, they were weak in the as-prepared samples, while the presence of absorbed water due to the nano-size, relatively low crystallinity is shown in Fig. 7. The bands of absorbed water were decreased as the calcination temperature increased. The characteristic bands for PO_4^{3-} appear at 474 cm^{-1} for the $v2$ mode, 963 cm^{-1} for the $v1$ mode [22]. The observation of the $v3$ symmetric P-O stretching vibration at 1,032/1,042 cm^{-1} as a distinguishable peak,

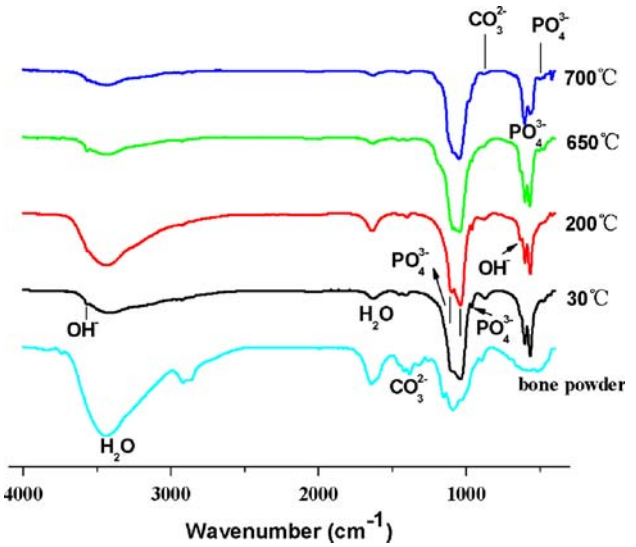

Fig. 7 FT-IR spectra of the human bone powder and the as-obtained powders

together with the bands 566/602 cm^{-1} corresponding to $v4$ bending vibration indicates the presence of HAP in the samples [27]. Three weak peaks at 872, 1,405, and 1,456 cm^{-1} are attributed to carbonate vibration [22, 32], which indicate the carbonate substitution in apatite crystals, and still exist in spite of high temperature treatment. The presence of carbonate was attributed to a reaction between atmospheric carbon dioxide and high solution pH during the preparation [22, 32], which consequently substituted OH^- group for CO_3^{2-} one. Thus, the presence of carbonates in HAP is desirable for medical application due to its similarity to the composition of biological apatite in the human bone. No detectable peaks belong to organic phase can be found. In Comparison with the as-prepared samples, the characteristic bands for OH^-, PO_4^{3-}, and CO_3^{2-} of the human bone powders have obviously shift and weakened, for bone is basically a composite of HAP and collagen.

Conclusion

In the cyclohexane—TX-100 and 1-pental—$CaCl_2$ aqueous solution system, nano-size well-dispersing HAP particles have been synthesized using a reverse microemulsion method without further calcination processing. The reactor systems with aqueous/organic volumetric ratios 1:10, 1:5, 2:5, and 1:2 were carefully selected for the microemulsion processing by the pseudo-ternary phase diagram and the electric conductivity measurement of the emulsion. The effect of different aqueous/organic ratio on the morphology of HAP particle was discussed in detail. The morphology changed from spherical to rod shape when the volume ratios 1:10, 1:5, 2:5 of aqueous/organic in the emulsion were applied respectively. It was also observed that when the aqueous/organic volumetric ratio was 1:2, the aggregated particles occurred. According to the results of XRD patterns, EDX and FTIR spectra, the obtained HAP nanoparticles with 1.658 Ca/P atomic ratio and carbonate substitution is chemically similar to the human bone powder, despite of the aqueous/organic ratio.

Acknowledgements This work was supported by the national key project program of China (No.1999054306) and program of ministry of science and technology in China (2001AA625050) to Pro. Changren Zhou.

References

1. Aoki H (1994) In: Medical application of hydroxyapatite. IShiyaku EuroAmerica Inc., Tokyo, St.Loui p 10
2. Hench LL (1991) J Am Ceram Soc 74:1487
3. Suchanek W, Yoshimura M (1998) J Mater Res 13:765
4. Takagi O, Kuramoto N, Ozawa M (2004) Ceram Int 30:139
5. Benmoussa A, Mikou M, Lacout JL, Siouffi AM (1995) J Chromatogr A 694:486
6. Jang KH, Song KB, Kim JS, Kim CH, Chung BH, Rhee SK (2000) Bioprocess Biosyst Eng 23:89
7. Lange FF (1989) J Am Ceram Soc 72:3
8. Ruys AJ, Wei M, Sorrelli CC, Dickson MR, Brandwood A, Milthorpe BK (1995) Biomaterials 16:409
9. Sonoda K, Furuzono T, Walsh D (2002) Solid State Ionics 151:32
10. Zhao F, Graysona WL, Ma T, Bunnellb B, Lu WW (2006) Biomaterials 27:1859
11. Sun JS, Wu YH, Lin FH (2005) Biomaterials 26:3953
12. Kim HW, Kim HE, Salih V (2005) Biomaterials 26:5221
13. Kokubo T, Kushitani H, Sakka S, Kitsugi T, Yamamuro T (1990) J Biomed Mater Res 24:721
14. Rao RR, Roopa HN, Kannan TS (1997) J Mater Sci Mater Med 8:511
15. Tas AC, Korkusuz F, Timicin M, Akkas N (1997) J Mater Sci Mater Med 8:91
16. Rhee SH, Tanaka J (1998) J Am Ceram Soc 81:3029
17. Wang F, Li MS, Lu YP, Qi YX (2005) Mater Lett 59:916
18. Ioku K, Kawachi G, Sasaki S (2006) J Mater Sci 41:1341. doi:10.1007/s10853-006-7338-5
19. Lim GK, Wang J, Ng SC, Gan LM (1996) Mater Lett 28:431
20. Koumoulidis GC, Katsoulds AP (2003) J Colloid Interface Sci 259:254
21. Bose S, Susanta KS (2003) Chem Mater 15:4464
22. Chen CW, Riman RE, Techuisen KS, Brown K (2004) J Cryst Growth 270:615
23. Guo GS, Sun YX, Wang ZH, Guo HY (2005) Ceram Int 31:869
24. Qi L, Ma JM, Cheng HM, Zhao ZG (1997) J Mater Lett 16:1779
25. Lam AC, Schechter RS (1987) J Colloid Interface Sci 120:42
26. Jillavenkatesa A, Condrate RA Sr (1998) J Mater Sci 33:4111. 10.1023/A:1004436732282doi:10.1023/A:1004436732282
27. Zhan YJ, Zheng CL, Liu YK, Wang GH (2003) Mater Lett 57:3265
28. Luo Q, Zhao XH, Zhou G (2004) Chem J Chinese U 25:1085
29. Lim GK, Wang J, Ng SC, Chew CH, Gan LM (1997) Biomaterials 18:1433
30. Lai C, Tang SQ, Wang YJ, Wei K (2005) Mater Lett 59:210
31. Layrolle P, Ito A, Tateishi T (1998) J Am Ceram Soc 81:1421
32. Kensaku S, Tsutomu F, Dominic W, Sato K, Tanaka J (2002) Solid State Ionics 151:321